PRODUCTION OF THE HL-LHC EXPERIMENTAL BEAM VACUUM CHAMBERS*

J. Sestak†, G. Bregliozzi, A. Galloro, M. Kukkola, F. Prizio, T. Raska, O. Santos, V. Baglin
European Organization for Nuclear Research, Geneva, Switzerland

Abstract

For the High-Luminosity LHC (HL-LHC) era following the third long shutdown (LS3 2026-2030), new generations of experimental vacuum chambers will be installed in the ATLAS, ALICE, CMS, and LHCb experiments. These chambers, located at the interaction points, ensure the required beam vacuum conditions while minimizing the impact of chamber materials on detector performance. The HL-LHC upgrade imposes tighter demands on mechanical precision, radiation tolerance, and surface quality to sustain higher beam currents, luminosity and radiation dose levels. Building on the experience gained during the LS2 exchange of the ALICE and CMS chambers, the LS3 designs introduce optimized materials, geometry, and production methods to meet these challenges. This contribution outlines the main design principles, manufacturing strategies, and qualification steps guiding the development of the LS3 experimental vacuum chambers for HL-LHC operation.

INTRODUCTION

During LS3 the experimental beam vacuum systems of ATLAS, ALICE, and CMS will undergo major upgrades to meet HL-LHC requirements. The baseline HL-LHC layout introduces new inner triplet assemblies at Points 1 and 5, absorbers for secondary particles produced in the collisions (TAXS) and upgraded vacuum assemblies for experiments (VAX) connecting the experimental beam vacuum sector via a gas injection system (GIS) to its ancillaries for pump-down, venting and diagnostics [1]. Furthermore, detector-specific upgrades dictate additional structural changes: ATLAS requires new beam vacuum chambers spanning ± 4 m from the interaction point (IP) to accommodate the new Inner Tracker (ITk) [2] and High Granularity Timing Detector (HGTD) [3], while ALICE's integration of their new Inner Tracking System (ITS3) [4] and a new Forward Calorimeter (FOCAL) [5] alters the vacuum layout from –9 m to +1 m from the IP.

DESIGN CONSIDERATIONS

The design of the particle accelerator beam vacuum chamber within the experimental areas shall follow requirements from both the experiment and the accelerator. Over the last two decades, a multi-domain design approach has been developed and implemented allowing a more comprehensive understanding of global design constraints and limitations.

Detector Requirements

Physics-motivated requirements for coverage and acceptance, together with general detector geometry, drive the main design parameters of the beam vacuum system. Tracker detectors, which form the innermost layer of the experiment, require chambers made of high-purity beryllium metal (> 98.5% Be) to minimize their impact on track reconstruction. Figure 1 shows a simplified integration of the ATLAS central chamber.

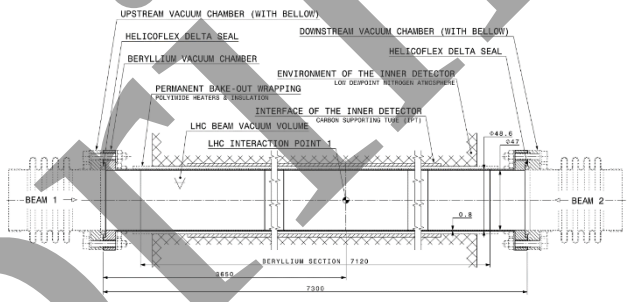

Figure 1: Integration of ATLAS central chamber.

Material budget presented to the detector within its spatial coverage, defined by the polar angle (pseudorapidity) η and the azimuthal angle φ directly contributes to its performance. The transparency of the vacuum system is a function of its geometry and the material of the chambers and expressed using the radiation length X_0 [6].

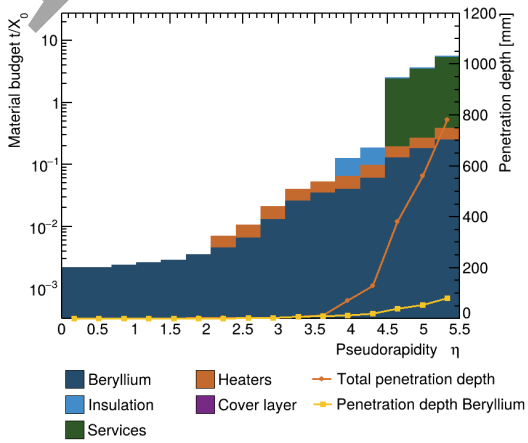

Figure 2: Contribution of ATLAS central chamber to material budget.

The contribution of the vacuum system to the material budget of the detector is shown by Fig. 2. It is defined as the ratio of penetration length during which the primary particle interacts with the chamber and its services. Permanent services present a non-negligible part of the material

* Work supported by the High Luminosity LHC Project
† josef.sestak@cern.ch

budget as the composition of the 5 mm thick bake-out wrapping may contain up to 18 different layers of material.

Material Properties in the Detector Environment

Vacuum chambers located outside of the zones with high transparency requirements are made of aluminium (AW-2219 and AW-5083). The radiation length of aluminium is a factor of 5 higher compared to stainless steel, as shown in Table 1, resulting in a lower dose for intervening personnel and a reduced background for the detector.

Table 1: Materials for Experimental Chambers

Material	**ρ** [g·cm^{-3}]	**X_0** [cm]	**E** [GPa]	**α** [10^{-6}·K^{-1}]
Aluminium	26.67	9.0	69	23.6
Beryllium	1.85	35.2	235	11.3
Stl. steel	8.0	1.8	195	16.0
Titanium	4.51	3.7	115	8.9

Challenging environmental conditions contribute to the following degradation mechanisms:

- Ageing of aluminium due to thermal cycles.
- Corrosion of aluminium while exposed to ambient air and the effect of cooling system.
- Radiation resistance of polymeric materials.

Aluminium AW-2219 T6 demonstrates excellent mechanical properties at elevated temperatures up to 250°C, which is mandatory for bake-out and activation of the non-evaporable getter (NEG) through thermal cycles. The temperature range used during commissioning reduces Young's modulus (by ~19% at 250°C), while the total time of the heating precipitates aging of the alloy and degradation of yield strength (decrease from 290 MPa to ~ 230 MPa) [7].

The presence of copper as the main alloying element of the 2219 aluminium reduces its corrosion resistance. The effect of the expected ambient conditions (relative humidity and temperature) shall be considered together with the adverse effect of the cooling system dewpoint.

The radiation resistance of organic materials, given the expected 20 MGy integrated dose over the HL-LHC lifetime, is a key factor in selecting appropriate materials for areas near the beam vacuum chambers. The qualified materials used for insulating the conductors of the permanent heating system are mainly polyimide (halogen free) with PEEK or Vesper for structural components.

Machine Aperture

The mechanical aperture of the system is specified to be the minimum acceptable diameter for the accelerator to safely inject, accelerate and collide beams. Aperture model calculations are performed using MAD-X for various beam modes and corresponding parameters such as Beam emittance, β*, beam dispersion, momentum offset and closed orbit excursion. For design purposes, the concept of mechanical aperture is expressed as the inscribed envelope, with its axis coinciding with the beam axis of the LHC physics coordinate system. This reference is then compared to the distorted physical aperture, which accounts for the full range of supporting systems, transverse offsets, survey errors, and calculated sagging [8].

Impedance

The concept of impedance Z(ω) presents one of the driving design constraints for the experimental vacuum system. The longitudinal impedance $Z_{\parallel}$ and transversal impedance $Z_{\perp}$ contribute to beam induced heating and beam instabilities affecting overall beam lifetime.

For the engineering design of the vacuum chambers, it is important to consider the presence of bellows, conical tapers (design rule < 15°) and the material of the walls and thin coatings. Assuming the interaction region contains two circulating beams in one aperture (bunch length 7.55 cm and spacing of 3.75 m), the thermomechanical simulations consider the presence of a linear heat source dissipating a power of ~ 1.4 – 2.9 W/m [9]. The effect cannot be neglected due to the permanent 5 mm aerogel insulation installed on the chambers. Increased heat load can lead to a local increase of outgassing and consequently a higher beam-gas background.

Structural Analysis

The analysis of the structural limits for the experimental beam vacuum chambers is performed via a loss of stability analysis. Vacuum chambers are long, thin-walled structures loaded by external pressure and prone to buckling.

Load types and their magnitude vary throughout the chamber's life-cycle stages and are shown in Table 2.

Table 2: Common Loads

Load type	**Production**	**Installation**	**Run**
Pressure	~1.5 bar	1 bar	1 bar
Thermal	RT - 250°C	RT - 200°C	-40°C-30°C
Inertial	Gravity	Gravity	Dynamic

Both linear and non-linear analysis is performed. Linear estimation of the shell critical pressure P_{cr} considers Young's modulus, Poisson's ratio of the chamber's material, the radius and the wall thickness [10].

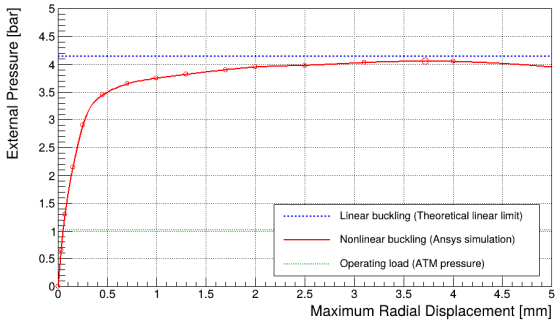

Figure 3: Comparison of linear and non-linear buckling.

The non-linear analysis shown in Fig. 3 a and includes the effects of geometrical imperfection and a variety of

other operational loads, allowing a better estimation of the critical point position (criterion $P_{cr} > 3$).

Dynamic analysis of the vacuum system includes a modal analysis to assess which natural frequencies to avoid, taking into account use-cases such as fast discharges of the experimental magnet, or seismic events.

Vacuum Requirements

Experimental beam vacuum chambers must meet a strict set of vacuum requirements for leak tightness, outgassing and surface quality [11]. To avoid the presence of vacuum pumps close to the sensitive physics regions, experimental vacuum sectors rely, by design, on the distributed pumping speed of NEG thin film coating. Systems are designed as full-metal, bakeable to 250°C and incorporating a surface quality ensuring full adhesion of the coating.

Detailed vacuum simulations, (example result shown in Fig. 4), ensure that the pressure requirements for molecular gas density are met for both static and dynamic conditions (including photon, electron and ion induced desorption, and beam pumping effects) [12].

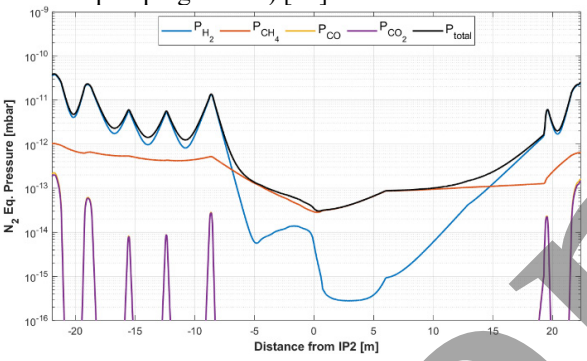

Figure 4: Pressure in IP2 (after beam conditioning).

The pressure stability of the system is a function of ion-induced desorption, pumping speed, and beam current. To avoid ion-induced instability, which occurs at the critical beam current I_c, the system must satisfy a criterion for the HL-LHC ultimate beam current ($I_c / 2 > 2 \cdot 1.09$ A).

ATLAS LAYOUT CASE STUDY

The design of the new forward region in the ATLAS experiment incorporates requirements from the Lucid detector, the HL-LHC VAX assembly and the interface with the new TAXS absorber. As shown in Fig. 5, the zone will be equipped with an assembly of two aluminium vacuum chambers. The VC1JE chamber (3105 mm long, internal diameter 80 mm, wall-thickness 1.1 mm) connects the existing chambers at 13.21 m from the IP1 and the VC1JI instrumented chamber (907 mm long; internal diameter 80 mm, wall thickness 1.5 mm), which is equipped with two ion sputter pumps (20 l·s^{-1}) and two Penning gauges. Both chambers will be equipped with a permanent heating system to avoid manual intervention in the vicinity of the TAXS absorber during bake-out [13].

The assembly will be supported via a cantilevered conical shell made of carbon fibre reinforced plastic, produced as a braided carbon fibre structure with injected radiation hard resin. Supporting mechanisms between the cone and the chambers are optimized for the physics coverage of the Lucid detector, offering high precision and fast adjustments during the technical stops.

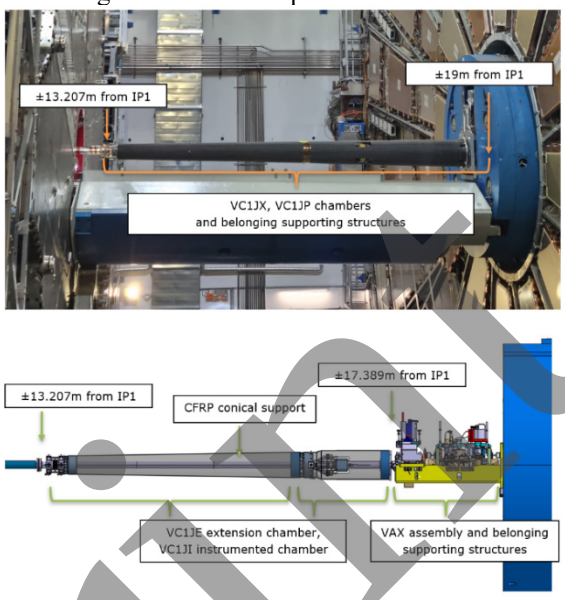

Figure 5: Layout changes in the ATLAS forward zone.

QUALIFICATION AND PRODUCTION

Experimental beam vacuum chambers are custom-built with unit prices often exceeding 100 kCHF, and lead times (assuming a mostly in-house production process) of between 12 – 24 months. Rigorous qualification is performed to avoid critical non-conformities (irreversible component damage) and to limit non-critical non-conformities during production process (see Fig. 6).

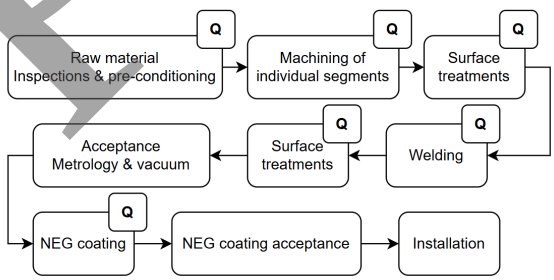

Figure 6: Production and qualification workflow.

The qualification strategy is based on both international standards (for example, ISO 10042 and ISO 13919 for weld quality) as well as internal guidelines and dedicated tests for cleaning efficiency [14] and coating adhesion [15].

CONCLUSION

This paper provides a summary of the design considerations, layout changes and production and qualification tasks of the experimental beam vacuum systems for the HL-LHC upgrade. A total of 13 optimised aluminium chambers, 3 aluminium-beryllium central chambers and 9 bellows compensators will be produced. These are foreseen to survive until the end of HL-LHC running, assuming operations from 2030 to 2041 and an ultimate luminosity 4000 fb^{-1}.

REFERENCES

[1] O. Aberle *et al.*, "High-Luminosity Large Hadron Collider (HL-LHC): Technical design report", CERN, Geneva, Switzerland, Rep. CERN-2020-010, 2020. doi:10.23731/CYRM-2020-0010

[2] ATLAS Collaboration, "Technical Design Report for the ATLAS Inner Tracker Pixel Detector", CERN, Geneva, Switzerland, Rep. CERN-LHCC-2017-021, ATLAS-TDR-030, Sep. 2017. doi:10.17181/CERN.FOZZ.ZP3Q

[3] ATLAS Collaboration, "Technical Design Report: A High-Granularity Timing Detector for the ATLAS Phase-II Upgrade", CERN, Geneva, Switzerland, Rep. CERN-LHCC-2020-007, ATLAS-TDR-031, Jun. 2020.

[4] ALICE Collaboration, "Technical Design report for the ALICE Inner Tracking System 3 - ITS3; A bent wafer-scale monolithic pixel detector", CERN, Geneva, Switzerland, Rep. CERN-LHCC-2024-003, ALICE-TDR-021, Feb. 2024.

[5] ALICE Collaboration, "Technical Design Report of the ALICE Forward Calorimeter (FoCal)", CERN, Geneva, Switzerland, Rep. CERN-LHCC-2024-004, ALICE-TDR-022, Feb. 2024.

[6] R. Jose Da Silva, "Calculation of radiation length in material", CERN, Geneva, Switzerland, Rep. PH-EP-Tech-Note-2010-013, Nov. 2025.

[7] J. G. Kaufman, "Properties and Applications of Wrought Aluminum Alloys", in *Properties and Selection: Aluminum Alloys*, vol. 2B, pp. 202 - 275, 2019. doi:10.31399/asm.hb.v02b.a0006543

[8] S. Lampaki, "Improved CERN LHC layout and aperture models", CERN, Geneva, Switzerland, Rep. CERN-THESIS-2024-19, Nov. 2024.

[9] E. Métral *et al.*, "Impedance and component heating", *Adv. Ser. Dir. High Energy Phys.*, vol. 24, pp. 269-280, 2015. doi:10.1142/9789814675475_0015

[10] S. P. Timoshenko and J. M. Gere, *Theory of Elastic Stability*, 2nd ed. New York, NY, USA: McGraw-Hill, 1963.

[11] P. Chiggiato, J. A. F. Somoza, and G. Bregliozzi, "Criteria for vacuum acceptance tests", CERN, Geneva, Switzerland, Rep. EDMS-1752123 v. 1.0.

[12] V. Baglin *et al.*, "Vacuum system", in *High-Luminosity Large Hadron Collider (HL-LHC): Technical design report*, CERN, Geneva, Switzerland, Rep. CERN-2020-010, 2020, ch. 12. doi:10.23731/CYRM-2020-0010.229

[13] J. Sestak, "LHC experimental beam vacuum systems ATLAS IP1 layout configuration for Run 4", presented at the TREX Meeting, CERN, Geneva, Switzerland, May 2025. [Online], https://indico.cern.ch/event/1543046/

[14] M. Taborelli, "Cleaning and Surface Properties", 2020. doi:10.48550/arXiv.2006.01585

[15] P. Costa Pinto, "Thin film coatings at CERN", CERN, Geneva, Switzerland, Rep. EDMS-11611437 v. 1.0.